AFSSAAE

Advances in Food Science, Sustainable Agriculture and Agroindustrial Engineering 2023 | Special Issue | 1-10
ISSN 2622-5921

ORIGINAL RESEARCH Open Access

Moringa leaf chlorophyll content measurement system based on optimized artificial neural network

Yusuf Hendrawan*, Titon Elang Perkasa, Joko Prasetyo, Dimas Firmanda Al-Riza, Retno Damayanti, Mochamad Bagus Hermanto, Sandra Sandra

Department of Biosystems Engineering, Faculty of Agricultural Technology, Universitas Brawijaya, Malang, Indonesia

KEYWORDS

Artificial neural network
Chlorophyll content
Machine vision
Moringa leaf

ABSTRACT

This research aimed to measure the chlorophyll content of Moringa leaves using machine vision and an optimized artificial neural network (ANN). A total of 480 images were used, 70% as training data and 30% as validation data. Features extraction was used to extract color and textural features. ANN was used as a modeling method, and the filter method was used as a feature selection method to optimize the best ANN input. Sensitivity analysis was done by varying the attribute evaluator in the filter method, as well as the learning function, the activation function, the learning rate, the momentum, the number of hidden layers, and the number of hidden nodes in the ANN. The best ANN structure was 10 input nodes, 30 nodes in the hidden layer 1, 40 nodes in the hidden layer 2, and 1 output node when using a learning rate of 0.1, a momentum of 0.5, the traincgf learning function, a logsig activation function in the hidden layer, and a tansig activation function in the output layer. The correlation coefficient between predicted and real data in the training process was 0.9792 with the training mean square error (MSE) of 0.0100, and the correlation coefficient of the validation process was 0.9794 with the validation MSE of 0.0099.

Introduction

Moringa plant (*Moringa oleifera*) has various benefits that are found in almost all parts of the plant, including the seeds, roots, leaves, and stems. Several studies have proven the benefits of Moringa plants as antihyperlipidemic, antidiabetic, immunomodulatory, antihypertensive, and gastrointestinal protection (Sharma et al., 2022). Moringa leaves contain chemical compounds i.e. amino acids in the form of glutamic acid, isoleucine, tryptophan, aspartic acid, alanine, arginine, histidine, valine, lysine, cysteine, phenylalanine, leucine, and methionine (Mahato et al., 2022). Moringa leaves also contain macro-elements such as potassium, calcium, magnesium, sodium, and phosphorus, as well as micro-elements such as zinc and manganese. Other parts of the Moringa plant such as roots, stems, and bark contain saponins and polyphenols (El-Hack et al., 2022). In addition, Moringa also contains flavonoids, reducing sugars, alkaloids, steroids, tannins, and essential oils. Moringa is also known to contain more than 40 antioxidants (Wang et al., 2022). The bioactive compounds in Moringa make it a high potential material in the pharmaceutical and food industries.

Bioactive compounds in plants can be identified from the chlorophyll content of leaves (Zepka et al., 2019). Chlorophyll is the main pigment in plants. Chlorophyll content indirectly has a relationship with vitamin C content and total polyphenols, so chlorophyll content measurement can also be used to identify vitamin C content and total polyphenols (Yaseen and Hajos, 2022). In general, there are two types of chlorophyll i.e. chlorophyll a and chlorophyll b. Chlorophyll pigments can absorb more blue (400-450 nm) and red (650-700 nm) light than green (500-600 nm) (Li and Olevano, 2022). Plants can get their energy needs from the red and blue spectrum, which is between 500 and 600 nm. So the green color of the leaves is caused by the absorption of red and blue light and the reflection of green light by chlorophyll (Lysenko et al., 2021). The content of chlorophyll in leaves varies from one plant to another. In addition to leaf age and variety, chlorophyll content also varies due to leaf position in one plant (Zhuang et al., 2021). The formation of

*Corresponding author
E-mail address: yusuf_h@ub.ac.id

chlorophyll in leaves is most affected by sunlight, but the age of the leaves also affects the levels of chlorophyll contained in the leaves.

Leaf chlorophyll pigment can be determined qualitatively and quantitatively. Qualitatively, leaf chlorophyll pigment can be detected by chromatographic method, colorimetric method, or by UV spectrophotometer (Wang et al., 2022). However, these methods of measuring leaf chlorophyll content have the disadvantage of being destructive to the object being measured. The use of a chlorophyll meter is preferred because it provides easy and fast measurement of chlorophyll, without destructing the leaf sample. The Konica Minolta SPAD-502 Plus chlorophyll meter can quantify chlorophyll content by measuring leaf absorbance in two wavelength regions (Brown et al., 2022). However, the use of this tool is still relatively expensive. Therefore, a non-destructive, accurate, but inexpensive method of measuring chlorophyll content is needed.

The development of computer vision methods and artificial neural network (ANN) modeling as non-invasive sensing can be used as alternative methods for measuring biological objects (Hendrawan et al., 2019a; Patricio and Rieder, 2018). The research of Hendrawan et al. (2018) and Hendrawan et al. (2019c) have successfully used machine vision and ANN methods to predict nitrogen content in spinach leaves. The results of the ANN model show a very high prediction accuracy with a mean square error (MSE) of 0.0000083 and a correlation coefficient R^2 between real and predicted data of 0.99. Hendrawan and Al Riza (2016) have also proven the effectiveness of computer vision and ANN in identifying water content in plants. The best ANN model uses 45 image features that produce the lowest root mean square error (RMSE) of 8.26×10^{-3} on testing-set data.

The combination of computer vision and ANN has also proven its effectiveness in predicting chlorophyll content in several types of plants. Suo et al. (2010) have investigated the effectiveness of using computer vision and ANN to predict the chlorophyll content of cotton plants. The results show a fairly high accuracy with an error value of 8.41%. Zhang et al. (2021) also tested computer vision and ANN methods to predict maize chlorophyll content. The results showed a fairly high accuracy with the highest RMSE value for training data of 0.08 and validation data of 0.11. Palumbo et al. (2022) used a computer vision system to predict total chlorophyll in fresh-cut rocket leaves (packaged and unpackaged). The results showed the effectiveness of computer vision in predicting total chlorophyll with RMSE values of 0.75 and R^2 0.77 on packaged rocket leaves and RMSE values of 0.70 and R^2 0.80 on unpackaged rocket leaves. Saha and Sasse (2022) estimate the chlorophyll content in bananas using a laser scanner of light detection and ranging sensor (LiDAR). The highest accuracy value that can be achieved is 69% on the validation data. Qi et al. (2021) proved the effectiveness and superiority of computer vision and ANN compared to other methods in monitoring chlorophyll content in peanut leaves. Barman and Choudhury (2022) in their research used smartphone-based computer vision equipped with ANN modeling to predict chlorophyll content. The results showed high accuracy with an R^2 value of 0.88. Other studies related to the use of computer vision and ANN to measure chlorophyll content in corn plants with an R^2 value of 0.82 (Vesali et al., 2015) and potato plants with an R^2 value of 0.90 (Gupta and Pattanayak, 2017). In previous studies, there has never been a study using computer vision and artificial intelligence to predict the chlorophyll content of Moringa leaves. This study aimed to measure the chlorophyll content of Moringa leaves using computer vision and an optimized ANN.

Research Methods

The computer vision sensor used in the image acquisition process on Moringa leaves was the HP DeskJet 2130 Series Scanner (Contact Image Sensor 1200 × 1200 dpi) (Damayanti et al., 2021). The process of measuring the chlorophyll content in Moringa leaves used the Chlorophyll Meter SPAD 502. Features extraction was carried out using self-built software based on Visual Basic 6.0 (Hendrawan et al., 2019b). Features extraction aimed to extract color and textural features. Features selection in this study used the Waikato Environment for Knowledge Analysis (WEKA) 3.8 software (Mark et al., 2009). The ANN modeling algorithm used Matlab R2014a software (Mathworks, 2014). The Acer Aspire 4752 laptop (Intel Core i3, 2330M 2.20Ghz, 2GB DDR 3 memory) was used for data processing including features extraction, feature selection, and ANN modeling.

The Moringa leaf material was harvested from the Sidomulyo village, Batu city, East Java province, Indonesia. Image data collection were carried out at the Laboratory of Biosystems Mechatronics, Faculty of Agricultural Technology, Universitas Brawijaya, Indonesia. Determination of

chlorophyll content using leaf aging parameters which were divided into three categories i.e. upper leaves, middle leaves, and lower leaves. The number of Moringa leaves samples used in this study was 480 with a digital resolution of 112 × 112 pixels. The acquired leaf image was saved in Bitmap (BMP) format and then the color and textural features were extracted. The results of color features extraction included red-green-blue (RGB), hue-saturation-value (HSV), hue-saturation-lightness (HSL), and L*a*b (Fan et al., 2021). Meanwhile, the textural features included homogeneity, entropy, sum mean, energy, correlation, contrast, maximum probability, inverse difference moment, variance, and cluster tendency in each color space (Hendrawan and Murase, 2011). Therefore, the total image features that can be extracted were 121 features. Because the number of image features was too large, a feature selection method was required to select the best feature-subset combination.

The feature selection method used in this study was the filter method (Bommert et al., 2020). Attribute evaluators used in the filter method included Chi-Squared Attribute Evaluator, Correlation Attribute Evaluator, ReliefF Attribute Evaluator, and Gain Attribute Evaluator (Hendrawan et al., 2019d). The backpropagation neural network algorithm was used to optimize the ANN learning process (Kuang et al., 2022). Sensitivity analysis was done by varying several parameters such as learning rate, momentum value, number of hidden layers, number of nodes in the hidden layer, learning function, activation function, and maximum epoch of 10,000 with a minimum error of 0.01. MSE was used to test the accuracy of the ANN model, where the lower the MSE value, the higher the accuracy of the ANN model.

Results and Discussions

Table 1 shows the ranking results of image features using the filter method. The results showed 10 image features from each selected attribute evaluator which have been sorted by the largest weight. To get the best features subset, it is necessary to test each combination of image features using ANN modeling until the lowest validation error was obtained. The ANN modeling for this test used two hidden layers with each number of nodes i.e. 30 and 40. The tansig activation function was used in the hidden layer, while purelin was used in the output layer, the learning function used trainlm, the learning rate was 0.1, and the momentum was 0.5.

Table 2 shows the test results on the feature-subset combination using ANN modeling. The test results showed that the Chi-Squared Attribute Evaluator gave the highest performance with the lowest validation MSE of 0.0040 when using 10 feature-subset combinations as input in ANN modeling. The best feature-subset combinations included Lab_b energy, Lab_b entropy, Lab_b homogeneity, Lab_b inverse difference moment, Lab_b cluster tendency, RGB_R sum mean, Lab_b variance, Lab_a sum mean, HSL_L sum mean, and Lab_a variance. Figure 1 shows an example of an image of Moringa leaves at several levels of chlorophyll content, resulting in different image data. Figure 1a shows an example of a Moringa leaf image with a chlorophyll content of 26.5 CCI which produced a value of Lab_b energy = 0.077; Lab_b entropy = 1.315; Lab_b homogeneity = 0.8356; Lab_b inverse difference moment = 0.2909; Lab_b cluster tendency = 37.1493; RGB_R sum mean = 87.9918; Lab_b variance = 9.8158; Lab_a sum mean = 120.0899; HSL_L sum mean = 76.0524; and Lab_a variance = 29.8327. Figure 1b shows an example of a Moringa leaf image with a chlorophyll content of 43.4 CCI which produced a value of Lab_b energy = 0.1023; Lab_b entropy = 1.1968; Lab_b homogeneity = 0.8459; Lab_b inverse difference moment = 0.2664; Lab_b cluster tendency = 99.8022; RGB_R sum mean = 70.2764; Lab_b variance = 26.3969; Lab_a sum mean = 122.2159; HSL_L sum mean = 74.7122; and Lab_a variance = 25.8799. Figure 1c shows an example of a Moringa leaf image with a chlorophyll content of 43.6 CCI which produced a value of Lab_b energy = 0.0773; Lab_b entropy = 1.3434; Lab_b homogeneity = 0.8509; Lab_b inverse difference moment = 0.2571; Lab_b cluster tendency = 96.2651; RGB_R sum mean = 77.5508; Lab_b variance = 25.0506; Lab_a sum mean = 121.8351; HSL_L sum mean = 79,8350; and Lab_a variance = 26.8538. Figure 1d shows an example of a Moringa leaf image with a chlorophyll content of 52.9 CCI which produced a value of Lab_b energy = 0.1842; Lab_b entropy = 0.9637; Lab_b homogeneity = 0.8726; Lab_b inverse difference moment = 0.2231; Lab_b cluster tendency = 144.8989; RGB_R sum mean = 51.1707; Lab_b variance = 38.4663; Lab_a sum mean = 122.9411; HSL_L sum mean = 64.3305; and Lab_a variance = 24.62

Table 1. Ranking of image features by weight

No.	Attribute evaluator	Image features	Weight	Rank
1.	Chi-Squared Attribute Evaluator	Lab_b Energy	2048.0564	1
		Lab_b Entropy	1191.6279	2
		Lab_b Homogeneity	872.8171	3
		Lab_b Inverse difference moment	831.6387	4
		Lab_b Cluster tendency	712.269	5
		RGB_R Sum Mean	709.1332	6
		Lab_b Variance	693.7712	7
		Lab_a Sum Mean	693.0808	8
		HSL_L SumMean	682.4674	9
		Lab_a Variance	677.9857	10
2.	Correlation Attribute Evaluator	Lab_b Energy	0.2116	1
		Lab_b Entropy	0.1678	2
		HSL_S Correlation	0.159	3
		Hue Inverse	0.1437	4
		Lab_b Inverse difference moment	0.1387	5
		RGB_B Correlation	0.1368	6
		Hue Variance	0.1352	7
		RGB_G Sum Mean	0.1341	8
		HSV_V Correlation	0.1332	9
		HSV_V Sum Mean	0.1332	10
3.	ReliefF Attribute Evaluator	Lab_b Energy	0.5929	1
		Lab_b Entropy	0.43246	2
		Lab_b Sum Mean	0.42036	3
		Hue Correlation	0.40089	4
		RGB_G Sum Mean	0.39728	5
		HSV_V Sum Mean	0.39694	6
		Lab_L Sum Mean	0.39013	7
		Hue Sum Mean	0.38423	8
		RGB_R Sum Mean	0.38418	9
		Hue Cluster tendency	0.38209	10
4.	Gain Ratio Attribute Evaluator	Lab_b Energy	0.6285	1
		Lab_b Entropy	0.4776	2
		Lab_b Inverse difference moment	0.3484	3
		HSL_S Correlation	0.3272	4
		RGB_R Sum Mean	0.3244	5
		Lab_b Homogeneity	0.3239	6
		HSL_L Sum Mean	0.3108	7
		Hue Inverse difference moment	0.3099	8
		RGB_G Sum Mean	0.3098	9
		HSV_V Sum Mean	0.3096	10

(a) (b) (c) (d)

Figure 1. Example of digital images of Moringa leaves at several levels of chlorophyll: (a) 26.5 CCI; (b) 43.4 CCI; (c) 43.6 CCI; (d) 52.9 CCI.

Table 2. ANN modeling results using various combinations of features-subset.

No.	Attribute Evaluator	Input (feature rank)	MSE Training	MSE Validation
1.	-	All features (121 features)	0.0029	0.0313
2.	Chi-Squared Attribute Evaluator	1-2	0.0099	0.2617
		1-3	0.0098	0.1521
		1-4	0.0096	0.1773
		1-5	0.0086	0.0101
		1-6	0.0071	0.0069
		1-7	0.0078	0.0076
		1-8	0.0089	0.0109
		1-9	0.0072	0.0088
		1-10	0.0038	0.0040
2.	Correlation Attribute Evaluator	1-2	0.0099	0.2617
		1-3	0.0100	0.1330
		1-4	0.0100	0.0946
		1-5	0.0099	0.0265
		1-6	0.0095	0.0226
		1-7	0.0095	0.0108
		1-8	0.0095	0.0094
		1-9	0.0089	0.0097
		1-10	0.0082	0.0089
3.	ReliefF Attribute Evaluator	1-2	0.0099	0.2617
		1-3	0.0099	0.0099
		1-4	0.0098	0.0107
		1-5	0.0090	0.0094
		1-6	0.0096	0.0102
		1-7	0.0092	0.0095
		1-8	0.0055	0.0061
		1-9	0.0089	0.0090
		1-10	0.0098	0.0099
4.	Gain Ratio Attribute Evaluator	1-2	0.0099	0.2617
		1-3	0.0099	0.1713
		1-4	0.0099	0.0575
		1-5	0.0099	0.0098
		1-6	0.0099	0.0113
		1-7	0.0100	0.0114
		1-8	0.0086	0.0105
		1-9	0.0085	0.0085
		1-10	0.0077	0.0076

Table 3 shows the results of the sensitivity analysis of the learning function parameters. There were 11 combinations of learning functions i.e. traincgb, traingdm, traincgf, traingd, traingdx, traincgp, trainoss, trainrp, traingda, trainlm, and trainscg. Among the 11 learning functions, the ANN model with traincgf ranked first in the best performance for the chlorophyll content prediction of Moringa leaves. The lowest validation MSE result was 0.0095 with the highest validation correlation coefficient of 0.9803.

Table 4 is the result of the sensitivity analysis of the activation function. ANN prediction accuracy is also affected by the type of activation function. Determination of the optimal activation function was done by varying the activation function at the input layer to the hidden layer and from the hidden layer to the output layer by using the binary sigmoid (logsig), bipolar sigmoid (tansig), and linear (purelin) activation functions. These three activation functions were combined using the previously selected learning function i.e. traincgf. The results of sensitivity analysis showed that the activation function of logsig at the hidden layer and tansig at the output layer obtained the lowest validation MSE of 0.0095 with a validation correlation coefficient of 0.9803.

Determination of the best ANN structure was the main focus of this study to obtain optimal prediction model for Moringa leaf chlorophyll content. In this study, several parameters affect the ANN structure i.e. the number of hidden layers (1 and 2); number of nodes (10, 20, 30, and 40); and learning rate and momentum (0.1, 0.5, and 0.9).

Table 3. Sensitivity analysis based on learning function

Learning Function	R Training	R Validation	MSE Training	MSE Validation
Traincgb *(Conjugate Gradient BP with Powell – Beale Restart)*	0.9793	0.9797	0.0099	0.0098
Traincgf *(Conjugate BP with Fletcher Reeves Update)*	0.9793	0.9803	0.0099	0.0095
Traincgp *(Conjugate Gradient BP with Polak Ribiere Update)*	0.9792	0.9796	0.0100	0.0098
Traingd (*Gradient Descent BP*)	0.9829	0.9825	0.0100	0.0098
Traingda (*Gradient Descent with Adaptive Learning Rate BP*)	0.9792	0.9786	0.0100	0.0103
Traingdm (*Gradient Descent with momentum Adaptive Learning*)	0.97916195	0.978719002	0.01	0.0103
Traingdx (*Gradient Descent with Momementum Adaptive Learning*)	0.9792	0.9600	0.0100	0.0227
Trainlm (*Lavenberg Marquadt BP*)	0.9815	0.9467	0.0096	0.0274
Trainoss (*One Step Secant BP*)	0.9792	0.9601	0.0100	0.0333
Trainrp (*Resilient BP*)	0.9795	0.9441	0.0098	0.0330
Trainscg Scaled (*Conjugate Gradient BP*)	0.9793	0.9575	0.0099	0.0203

Table 4. Sensitivity analysis based on activation function

Learning Function	Activation Function			R Training	R Validation	MSE Training	MSE Validation
	Hidden Layer 1	Hidden Layer 2	Output Layer				
Traincgf	Tansig	Tansig	Purelin	0.9793	0.9792	0.0100	0.0101
	Tansig	Tansig	Tansig	0.9793	0.9791	0.0100	0.0100
	Tansig	Tansig	Logsig	0.9207	0.9156	0.0870	0.0886
	Logsig	Logsig	Purelin	0.9792	0.9786	0.0100	0.0103
	Logsig	Logsig	Tansig	0.9793	0.9803	0.0099	0.0095
	Logsig	Logsig	Logsig	0.9207	0.9158	0.0870	0.0894

Table 5. Sensitivity analysis based on ANN structure

Learning Rate	Momentum	ANN Structure	R training	R Validation	MSE Training	MSE Validation
0.1	0.5	10>>30>>1	0.9211	0.9121	0.0871	0.0920
		10>>40>>1	0.9207	0.9178	0.0871	0.0904
		10>>30>>40>>1	0.9792	0.9794	0.0100	0.0099
		10>>40>>30>>1	0.9792	0.9785	0.0100	0.0103
		10>>40>>40>>1	0.9792	0.9792	0.0100	0.0100
	0.9	10>>30>>1	0.9207	0.8966	0.0871	0.0922
		10>>40>>1	0.9209	0.9111	0.0870	0.0895
		10>>30>>40>>1	0.9796	0.9785	0.0100	0.0103
		10>>40>>30>>1	0.9793	0.9784	0.0100	0.0104
		10>>40>>40>>1	0.9794	0.9785	0.0100	0.0103

The best structure can be seen in Table 5, the structure of 10-30-40-1 with a learning rate of 0.1 and a momentum of 0.5 produced the lowest validation MSE of 0.0099. Through these results, it can be concluded that the best ANN structure used two hidden layers.

Figure 2 shows the performance of the learning process in ANN. The graph shows the relationship between the number of epochs and the MSE value during the training process on the best ANN model to predict the chlorophyll content in Moringa leaves. The results of the learning iteration

showed that the prediction error value continued to decrease significantly as the training iteration increased. The ANN learning process converged on the 169th iteration with an MSE value of 0.0099672. The training results reached the goal in the 47th iteration and stopped at the 169th iteration when the minimum error value was reached.

Figure 3 shows the regression plots for the training regression and validation regression. From the training regression plot image, the distribution between the target data and the predicted data showed a correlation coefficient of 0.97924. While the validation regression plot showed that there were fewer data that deviated from the linear fit line, causing the validation correlation coefficient to be slightly higher at 0.97941. Based on the results of the study, there was a strong relationship between image features as the ANN input and chlorophyll content of Moringa leaves as the ANN output with a correlation coefficient value closed to 1.

The best ANN structure (10-30-40-1) can be seen in Figure 4 which consisted of 10 neurons in the input layer (Lab_b energy, Lab_b entropy, Lab_b homogeneity, Lab_b inverse difference moment, Lab_b cluster tendency, RGB_R sum mean, Lab_b variance, Lab_a sum mean, HSL_L sum mean, and Lab_a variance), 30 nodes in the first hidden layer, 40 nodes in the second hidden layer and 1 node in the output layer (chlorophyll content of Moringa leaves). This best ANN structure produced the lowest MSE of 0.0099.

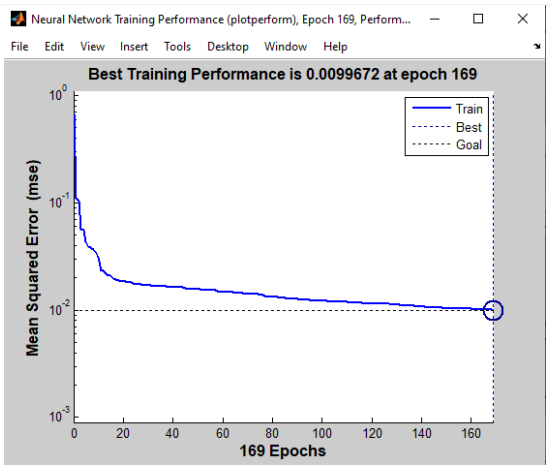

Figure 2. ANN training process performance

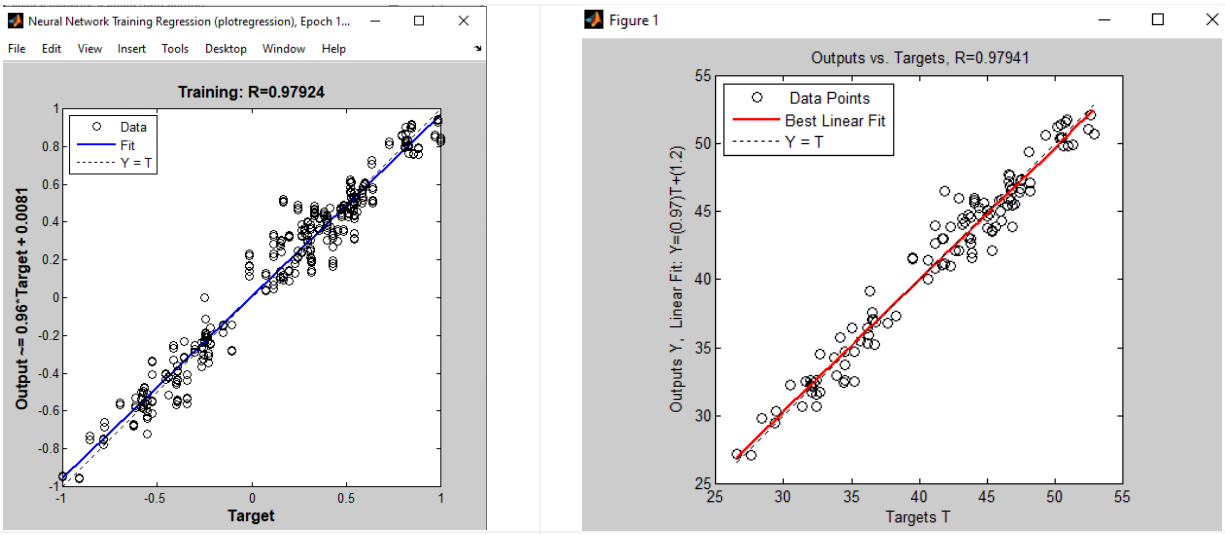

(a) (b)

Figure 3. Regression plots of the best ANN model simulation results: (a) training data; (b) validation data

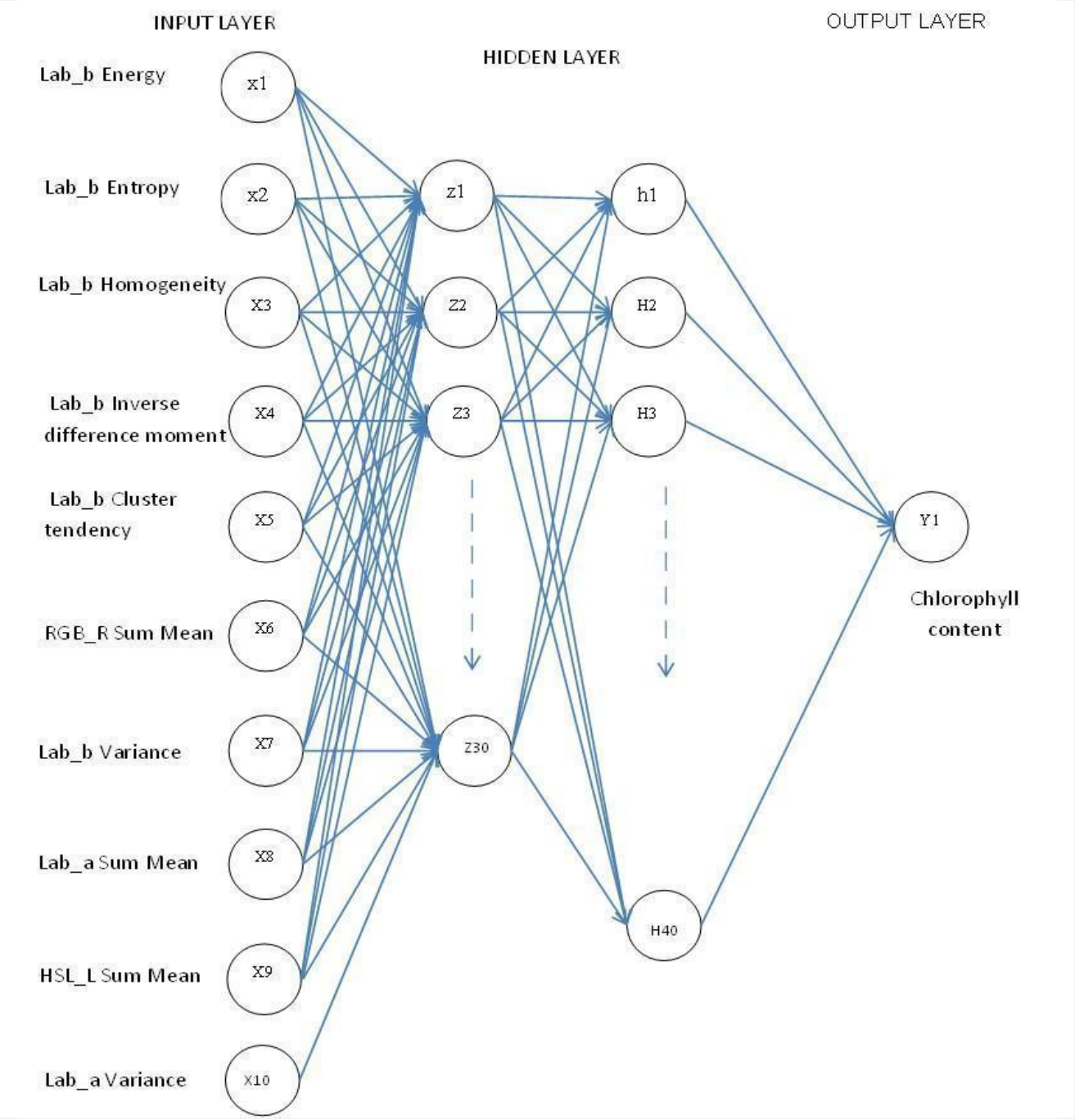

Figure 4. The best ANN structure for prediction of chlorophyll content of Moringa leaves

Conclusion

This study aimed to build ANN model to predict the chlorophyll content of Moringa leaves using computer vision. The filter method was used as feature selection to select the best combination of image features that can be used as ANN input. The Chi-Square method was chosen as the best attribute evaluator in the filter method. From the results of this feature selection, the 10 best image features were selected as ANN input i.e. Lab_b energy, Lab_b entropy, Lab_b homogeneity, Lab_b inverse difference moment, Lab_b cluster tendency, RGB_R sum mean, Lab_b variance, Lab_a sum mean, HSL_L sum mean, and Lab_a variance. Sensitivity analysis had also been carried out to obtain the best ANN model structure i.e. 10-30-40-1 (10 nodes in the input layer, 30 nodes in the first hidden layer, 40 nodes in the second hidden layer, and 1 node in the output layer), traincgf as learning function, logsig as an activation function in the hidden layer, and tansig as an activation function in the output layer. The selected ANN structure produced a training correlation coefficient of 0.9792, a validation correlation coefficient of 0.9794, a training MSE of 0.0100, and a validation MSE of 0.0099.

Suggestions from this study are the implementation of the ANN model on a computer vision-based measuring instrument to predict the chlorophyll content of Moringa leaves. This computer vision-based measuring instrument has the advantages of being non-destructive, simple, low-cost, real-time, and accurate

Acknowledgement
Authors wishing to acknowledge support and funding from the Professor Research Grants Program, Faculty of Agricultural Technology, Universitas Brawijaya.

Declarations

Conflict of interests The authors declare no competing interests.

References

Barman, U., and Choudhury, R. D. (2022) 'Smartphone image based digital chlorophyll meter to estimate the value of citrus leaves chlorophyll using Linear Regression, LMBP-ANN and SCGBP-ANN', *Journal of King Saud University - Computer and Information Sciences*, 34 (6), pp. 2938-2950

Bommert, A., Sun, X., Bischi, B., Rahnenfuhrer, J., and Lang, M. (2020) 'Benchmark for filter methods for feature selection in high-dimensional classification data', *Computational Statistics & Data Analysis*, 143, pp. 106839

Brown, L. A., Williams, O., and Dash, J. (2022) 'Calibration and characterisation of four chlorophyll meters and transmittance spectroscopy for non-destructive estimation of forest leaf chlorophyll concentration', *Agricultural and Forest Meteorology*, 323, pp. 109059

Damayanti, R., Rachma, N., Al Riza, D. F., and Hendrawan, Y. (2021) 'The prediction of chlorophyll content in african leaves (*Vernonia amygdalina Del.*) using flatbed scanner and optimised artificial neural network', *Journal of Science & Technology*, 29 (4), pp. 2509 - 2530

El-Hack, M. E. A., Alqhtani, A. H., Swelum, A. A., El-Saadony, M. T., Salem, H. M., Babalghith, A. O., Taha, A. E., Ahmed, O., Abdo, M., and El-Tarabily, K. A. (2022) 'Pharmacological, nutritional and antimicrobial uses of *Moringa oleifera Lam.* leaves in poultry nutrition: an updated knowledge', *Poultry Science*, In Press. Available at https://doi.org/10.1016/j.psj.2022.102031 (Accessed: 27 June 2022)

Fan, Y., Li, J., Guo, Y., Xie, L., and Zhang, G. (2021) 'Digital image colorimetry on smartphone for chemical analysis: A review digital image colorimetry on smartphone for chemical analysis: A review', *Measurement*, 171, pp. 108829

Gupta, S. D., and Pattanayak, A. K. (2017) 'Intelligent image analysis (IIA) using artificial neural network (ANN) for non-invasive estimation of chlorophyll content in micropropagated plants of potato', *In Vitro Cellular & Developmental Biology - Plant*, 53, pp. 520-526

Hendrawan, Y., and Al Riza, D. F. (2016) 'Machine vision optimization using nature-inspired algorithms to model sunagoke moss water status', *International Journal on Advanced Science, Engineering and Information Technology*, 6 (1), pp. 45-57

Hendrawan, Y., Amini, A., Maharani, D. M., and Sutan, S. M. (2019a) 'Intelligent non-invasive sensing method in identifying coconut (*Coco nucifera var. Ebunea*) ripeness using computer vision and artificial neural network', *Pertanika Journal of Science & Technology*, 27 (3), pp. 1317 - 1339

Hendrawan, Y., Fauzi, M. R., Khairunnisa, N. S., Andreane, M., Hartianti, P. O., Halim, T. D., and Umam, C. (2019b) 'Development of colour co-occurrence matrix (CCM) texture analysis for biosensing', *IOP Conference Series: Earth and Environmental Science*, 230, pp. 012022

Hendrawan, Y., Hawa, L. C., and Damayanti, R. (2018) 'Fish swarm intelligent to optimize real time monitoring of chips drying using machine vision', *IOP Conference Series: Earth and Environmental Science*, 131, pp. 012020

Hendrawan, Y., and Murase, H. (2011) 'Neural-intelligent water drops algorithm to select relevant textural features for developing precision irrigation system using machine vision', *Computers and Electronics in Agriculture*, 187, pp. 106272

Hendrawan, Y., Sakti, I. M., Wibisono, Y., Fauzy, M. R., Umam, C., and Sutan, S. M. (2019c) 'Intelligent precision nitrogen fertilizer application based on speaking plant approach for environmental sustainability', *IOP Conference Series: Earth and Environmental Science*, 239, pp. 012027

Hendrawan, Y., Sakti, I. M., Wibisono, Y., Rachmawati, M., and Sutan, S. M. (2018) 'Image Analysis using Color Co-occurrence Matrix Textural Features for Predicting Nitrogen Content in Spinach', *TELKOMNIKA*, 16 (6), pp. 2712-2724

Hendrawan, Y., Widyaningtyas, S.,and Sucipto, S. (2019d) 'Computer vision for purity, phenol, and pH detection of luwak coffee green bean', *TELKOMNIKA*, 17 (6), pp. 3073-3085

Kuang, F., Long, Z., Kuang, D., Liu, X., and Guo, R. (2022) 'Application of back propagation neural network to the modeling of slump and compressive strength of composite geopolymers', *Computational Materials Science*, 206, pp. 111241

Li, J., and Olevano, V. (2022) 'Bethe-Salpeter equation insights into the photo-absorption function and exciton structure of chlorophyll a and b in light-harvesting complex II', *Journal of Photochemistry and Photobiology B: Biology*, 232, pp. 112475

Lysenko, V., Kosolapov, A., Usova, E., Tatosyan, M., Vardunny, T., Dmitriev, P., Rajput, V., Krasnov, V.,and Kunitsina, A. (2021) 'Chlorophyll fluorescence kinetics and oxygen evolution in Chlorella vulgaris cells: Blue vs. red light', *Journal of Plant Physiology*, 258-259, pp. 153392

Mahato, D. K., Kargwal, R., Kamle, M., Sharma, B., Pandhi, S., Mishra, S., Gupta, A., Mahmud, M. M. C., Gupta, M. K., Singha, L. B., and Kumar, P. (2022) 'Ethnopharmacological properties and Nutraceutical potential of *Moringa oleifera*', *Phytomedicine Plus*, 2 (1), pp. 100168

Mark, H., Eibe, F., Geoffrey, H., Bernhard, P., Peter, R., Ian, H.W. (2009) 'The WEKA Data Mining Software: An Update', *SIGKDD Explorations*, 11 (1)

Mathworks. (2014) MATLAB Release 2014a. http://www.mathworks.com.

Palumbo, M., Pace, B., Cefola, M., Montesano, F.F., Colelli, G., and Attolico, G. (2022) 'Non-destructive and contactless estimation of chlorophyll and ammonia contents in packaged fresh-cut rocket leaves by a computer vision system', *Postharvest Biology and Technology*, 189, pp. 111910

Patricio, I. D., and Rieder, R. (2018) 'Computer vision and artificial intelligence in precision agriculture for grain crops: A systematic review', *Computers and Electronics in Agriculture*, 153, pp. 69-81

Qi, H., Wu, Z., Zhang, L., Zhou, J., Jun, Z., and Zhu, B. (2021) 'Monitoring of peanut leaves chlorophyll content based on drone-based multispectral image feature extraction', *Computers and Electronics in Agriculture*, 187, pp. 106292

Saha, K. K., and Sasse, M. Z. (2022) 'Estimation of chlorophyll content in banana during shelf life using LiDAR laser scanner', *Postharvest Biology and Technology*, 192, pp. 112011

Sharma, K., Kumar, M., Waghmare, R., Suhag, R., Gupta, O. P., Lorenzo, J. M., Prakash, S., Rais, N., Sampathrajan, V., Thappa, C., Anitha, T., Sayed, A. A. S., Abdel-Wahab, B. A., Senapathy, M., Pandiselvam, R., Dey, A., Dhumai, S., Amarowicz, R., and Kennedy, J. F. (2022) 'Moringa (Moringa oleifera Lam.) polysaccharides: Extraction, characterization, bioactivities, and industrial application', *International Journal of Biological Macromolecules*, 209, pp. 763-778

Suo, X. M., Jiang, Y. T., Li, S. K., Wang, K., and Wang, C. T. (2010) 'Artificial neural network to predict leaf population chlorophyll content from cotton plant images', *Agricultural Sciences in China*, 9 (1), pp. 38 - 45

Vesali, F., Omid, M., Kaleita, A., and Mobli, H. (2015) 'Development of an android app to estimate chlorophyll content of corn leaves based on contact imaging', *Computers and Electronics in Agricultur*, 116, pp. 211-220

Wang, G., Zeng, F., Song, P., Sun, B., Wang, Q., and Wang, J. (2022) 'Effects of reduced chlorophyll content on photosystem functions and photosynthetic electron transport rate in rice leaves', *Journal of Plant Physiologyology*, 272, pp. 153669

Wang, Y. Y., Peng, C., Zhang, Y., Wang, Z. R., Chen, Y. M., Dong, J. F., Xiao, M. L., Li, D. L., Li, W., Zou, Q. J., Zhang, K., and Wei, P. (2022) 'Optimization, identification and bioactivity of flavonoids extracted from Moringa oleifera leaves by deep eutectic solvent', *Food Bioscience*, 47, pp. 101687

Yaseen, A. A., and Hajos, M. T. (2022) 'Evaluation of moringa (*Moringa oleifera Lam.*) leaf extract on bioactive compounds of lettuce (*Lactuca sativa L.*) grown under glasshouse environment', *Journal of King Saud University - Science*, 34 (4), pp. 101916

Zepka, L. Q., Lopes, E. J., and Roca, M. (2019) 'Catabolism and bioactive properties of chlorophylls', *Current Opinion in Food Science*, 26, pp. 94-100

Zhang, L., Han, W., Niu, Y., Chavez, J. L., Shao, G., and Zhang, H. (2021) 'Evaluating the sensitivity of water stressed maize chlorophyll and structure based on UAV derived vegetation indices', *Computers and Electronics in Agriculture*, 185, pp. 106174

Zhuang, J., Zhou, L., Wang, Y., and Chi, Y. (2021) 'Nitrogen allocation regulates the relationship between maximum carboxylation rate and chlorophyll content along the vertical gradient of subtropical forest canopy', *Agricultural and Forest Meteorology*, 307, pp. 108512